Available online at www.sciencedirect.com
SCIENCE DIRECT®
Optics Communications 215 (2003) 191–197
OPTICS COMMUNICATIONS
www.elsevier.com/locate/optcom

Phase-matched nonlinear interactions in a holey fiber induced by infrared super-continuum generation

Luca Tartara[a,*], Ilaria Cristiani[a], Vittorio Degiorgio[a,1], Fabrizio Carbone[b], Daniele Faccio[b], Marco Romagnoli[b], Walter Belardi[c]

[a] *Istituto Nazionale per la Fisica della Materia and Dipartimento di Elettronica, Università di Pavia, Via Ferrata 1, I-27100 Pavia, Italy*
[b] *Pirelli Labs-Optical Innovation, viale Sarca 222, I-20126 Milano, Italy*
[c] *Optoelectronics Research Center, University of Southampton, Southampton SO17 1BJ, UK*

Received 10 July 2002; received in revised form 10 October 2002; accepted 13 November 2002

Abstract

By coupling 110-fs pulses at $\lambda = 1.55\,\mu m$ into a 45-cm-long holey fiber, we observe the generation of a broadband continuum, followed by the appearance of a sharp blue line at 430 nm. Blue light is generated in a high-order mode by a third-harmonic generation process that is phase-matched with the super-continuum component at 1.29 μm. Such an interpretation is supported by measurements performed by using 1.29-μm pulses and also by simulation. In addition we find that the choice of an input polarization tilted with respect to the fiber-birefringence axis can lead to the generation of new frequencies through a four-wave mixing process that exploits non-diagonal components of the third-order susceptibility.

PACS: 42.65; 42.65.R; 42.65.W; 42.65.H; 42.65.K

Keywords: Holey fibers; Nonlinear optics in fibers; Ultrashort pulse propagation in fibers; Third-harmonic generation; Four-wave mixing; Super-continuum generation

1. Introduction

Holey fibers (HFs), that is, fibers containing an air-silica microstructure, are very attractive for the realization of all-optical fiber devices based on nonlinear phenomena because the large refractive-index step between silica and air allows light to be confined into a very small area, resulting in enhanced nonlinear effects [1–6]. The generation of a broadband supercontinuum in an HF was first observed by Ranka et al. [2] with 100-fs 790-nm input pulses, and was subsequently studied in some detail by using various pulse durations and input wavelengths [3–6]. Omenetto et al. [7] reported the observation of third-harmonic generation (THG) and no supercontinuum by using 170-fs 1550-nm input pulses. In addition, recent

* Corresponding author. Tel.: +39-0382-505-595; fax: +39-0382-422-583.
E-mail addresses: tartara@ele.unipv.it (L. Tartara), v.degiorgio@ele.unipv.it (V. Degiorgio).
[1] Also corresponding author. Tel.: +39-0382-505-208; fax: +39-0382-422-583.

0030-4018/02/$ - see front matter
PII: S0030-4018(02)02194-6

works describe the soliton fission phenomena occurring near the zero-dispersion wavelength of the holey fiber [8,9]. The available results indicate that various phenomena can occur and compete when ultrashort pulses propagate in highly nonlinear holey fibers. In order to reach a more complete understanding of the different mechanisms and of their connection with the fiber microstructure, it is important to perform a wide exploration of the phenomenology of the nonlinear effects occurring in HFs.

In this paper, we describe an experiment performed with 110-fs pulses at 1550 and 1290 nm, in which, by increasing progressively the input power, we observe first the generation of a broad continuum and successively the appearance in the output spectrum of an intense sharp line at 430 nm that can be attributed to a THG process. We also find that the choice of an input polarization tilted with respect to the fiber-birefringence axis can lead to the generation of a new line at 890 nm through a phase-matched four-wave mixing process that uses a frequency extracted from the supercontinuum and exploits non-diagonal components of the third-order susceptibility. Unlike most part of the existing literature, we focus the discussion on the interpretation of the sharp lines appearing in the output spectrum. In particular, we treat the phase-matched generation of third-harmonic radiation by using the results of a systematic numerical simulation of the modal properties of the used fiber and we propose an explanation for the fact that a significant THG is not commonly found in nonlinear experiments involving holey fibers. Furthermore, we discuss the phase-matching condition for the four-wave mixing process, pointing out the role of the fiber birefringence.

2. Experimental results

The used HF was fabricated at the Optoelectronics Research Center (Southampton, UK), and has the structure shown in Fig. 1. It is characterized by a very small core diameter (about 1.5 μm) that enhances its nonlinear properties. As discussed in [1,5], the asymmetry in the core region induces a high birefringence leading to a polarization maintaining behavior. Our experimental results are obtained by coupling a 110-fs transform-limited pulse train (80 MHz repetition rate) generated by an optical parametric oscillator (OPO) into a 45-cm-long HF span. The first set of measurements was carried out by tuning the OPO at 1.55 μm. The input light was linearly polarized along one of the principal polarization axes of the HF that we call the z-axis. The results here described all refer to situations in which the input radiation is coupled to the fiber fundamental mode. In our experiment we measure the total optical power at the fiber output. This is only slightly smaller than the power coupled inside the fiber, taking into account that the linear attenuation coefficient of our fiber in the region 1300–1600 nm is around 0.6 m^{-1}. The maximum power measured at the fiber output was about 40 mW. By increasing progressively the input power we observed the onset of stimulated Raman radiation followed by a progressive broadening of the spectrum due to four-wave mixing and self-phase modulation. Some output spectra are shown in Fig. 2. When the average input power exceeds 25 mW, a sharp line due to blue light at a wavelength around 430 nm appears in the output spectrum. The blue light has a complicated near-field spatial pattern, shown in Fig. 3, constituted of several lobes indicating the presence of high-order modes. In addition to the 430-nm line, the optical spectra

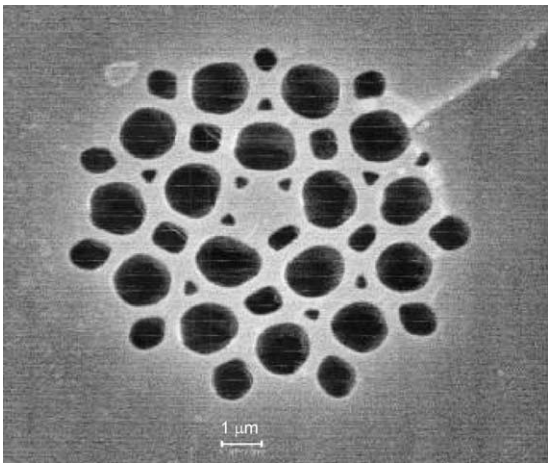

Fig. 1. Scanning-electron microscope photograph of the holey fiber.

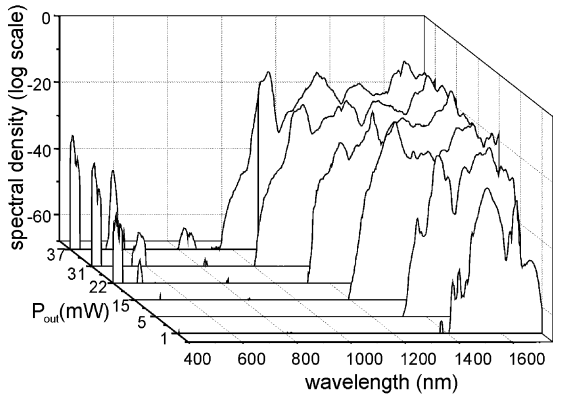

Fig. 2. A family of output spectra obtained by launching 110-fs pulses at $\lambda = 1550$ nm with increasing input power.

of Fig. 2 present also two much weaker lines at $\lambda = 517$ nm, corresponding to the third harmonic of the input beam, and at $\lambda = 570$ nm, corresponding to the third harmonic of a Raman shifted frequency. The first observation of THG in higher-order modes of a holey fiber was made by Ranka et al. [10]. Subsequently Omenetto et al. [7] performed a detailed THG experiment, showing the generation of a rather intense third harmonic of 1550-nm light. On the contrary, in our case, the main effect observed at 1550 nm is spectral broadening. Only when the spectral broadening reaches the appropriate wavelength range, a significant THG is produced. As discussed below, numerical simulation confirms that the third-harmonic generation process can be phase-matched through modal dispersion.

In order to obtain further information about the mechanism of generation of the spectral line at 430 nm, we have tuned the OPO at 1.29 μm. Two of the spectra obtained with an input polarization parallel to the z-axis are shown in Fig. 4. In this situation, by increasing progressively the input power, we find that the first observed nonlinear effect is third-harmonic generation at the same wavelength (430 nm) and with the same spatial pattern observed with the 1.55-μm input. The bandwidth of the blue radiation is narrower than 0.5 nm. The efficiency for generation of blue light is in this case much larger than that found with the 1.55-μm input. By measuring the output power of blue light, P_{430}, as a function of the input power P_{1290}, we find, at low input intensity, a cubic dependence. The maximum observed conversion efficiency $\eta = P_{430}/P_{1290}$ was about 0.2%.

From the comparison of the spectra taken at same input power (see Figs. 2 and 4(b)) it can be noticed that the wave-mixing effect responsible for super-continuum generation is less efficient when starting from 1.29 μm. This is consistent with the fact that our numerical simulations, discussed in the next section, predict a larger value of the group velocity dispersion at 1.29 μm with respect to 1.55 μm.

Very interesting effects are observed when the linear polarization of the input beam is rotated by an angle θ with respect to the z-axis. If θ is varied from 0° to 90° by keeping fixed the input power, we observe that the intensity of the blue line decreases and reaches a minimum around 45°, recovering the full value when the linear polarization

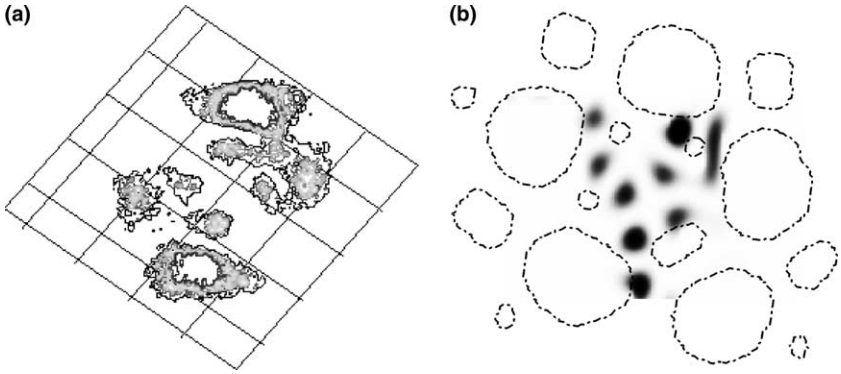

Fig. 3. Near-field intensity pattern of the high-order mode at 430 nm: comparison between experimental observation (a) and numerical simulation (b). The central part of the fiber structure is shown as a background of the numerical simulation pattern.

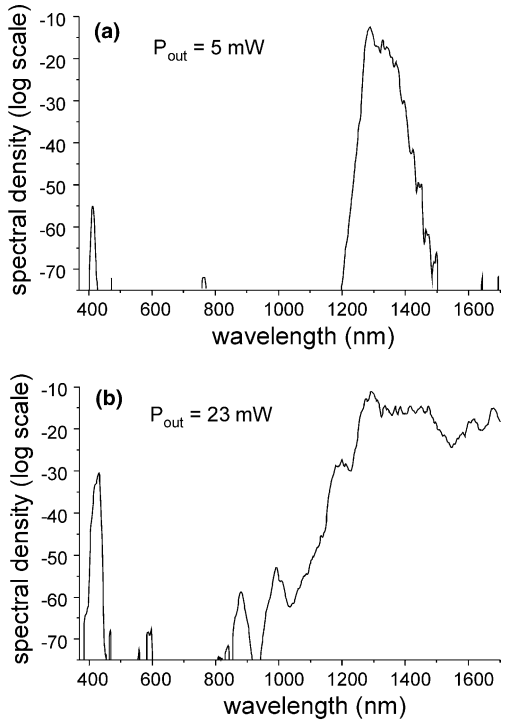

Fig. 4. Output spectra obtained by launching 110-fs pulses at $\lambda = 1290$ nm at two different values of the input power.

becomes parallel to the x-axis ($\theta = 90°$). We find that the wavelength of blue light shifts from 430 to 415 nm as θ is varied from 0° to 90°. Such an effect can be ascribed to the modified phase-matching condition due to fiber birefringence. We also find that, by rotating the input polarization, a new line centered at 890 nm is generated in the output spectrum, as shown in Fig. 5. The spectra reported in Fig. 5 are relative to measurements performed at 1290 nm, but similar results were obtained also at 1550 nm. In both cases the 890-nm line appears when the spectral broadening extends down to the wavelength range 1100–1150 nm. As discussed in detail in Section 3, we attribute the origin of such a peak to a four-wave mixing process that uses two wavelengths extracted from the supercontinuum. The fact that the new line at 890 nm becomes evident only when the input polarization is not parallel to a principal axis of the HF is a clear indication that an off-diagonal component of $\chi^{(3)}$ is involved. We see from Fig. 5 that the maximum amplitude of the 890-nm peak corresponds to an

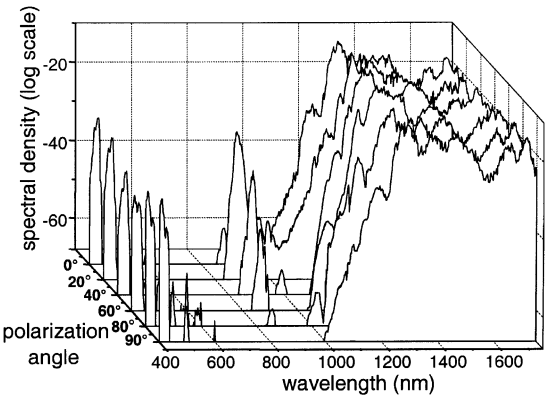

Fig. 5. A family of output spectra obtained by launching 110-fs pulses at $\lambda = 1290$ nm at fixed input power ($P_{1290} = 20$ mW at the fiber output) and variable direction of polarization θ.

intermediate value of θ, around 35°. We have also measured the polarization of 890-nm light, and found that it is linearly polarized along the x-axis.

3. Discussion

3.1. Third-harmonic generation

We simulated the modal behavior of our HF by using a software program (BPM *RSOFT*) based on the beam-propagation method. The grid included 528×246 pixels, with a pixel size of 50 nm. As input profile for the simulation we used the real fiber section shown in Fig. 1. Let us call n_λ^m the effective index of refraction for the mth mode at the wavelength λ. We performed the calculation of n_λ^m for the fundamental mode ($m = 1$) in the wavelength range 350–1700 nm. The calculated behavior of the effective index and of the group velocity dispersion (GVD) parameter as functions of wavelength is given in Fig. 6. We also derived the values of n_λ^m at the two wavelengths 1290 and 430 nm for $m = 1, \ldots, 20$. The results are shown in Fig. 7. We find that the phase matching condition for THG can be satisfied by taking the fundamental mode at $\lambda_p = 1290$ nm and the 14th-order mode at 430 nm, that is, $n_{1290}^1 = n_{430}^{14} = 1.387$. The 14th-order mode has a transverse spatial structure characterized by several lobes (see Fig. 3). Some similarity exists with the experimental one.

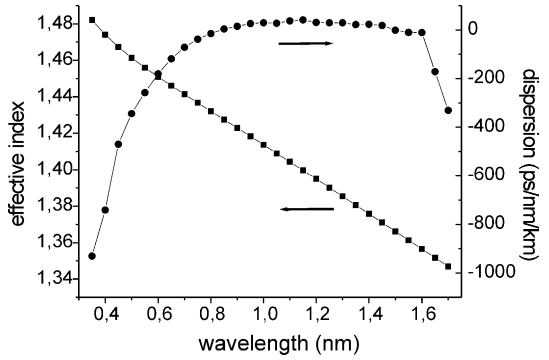

Fig. 6. Calculated values of the effective index and dispersion parameter as functions of wavelength for the fundamental mode of the holey fiber shown in Fig. 1.

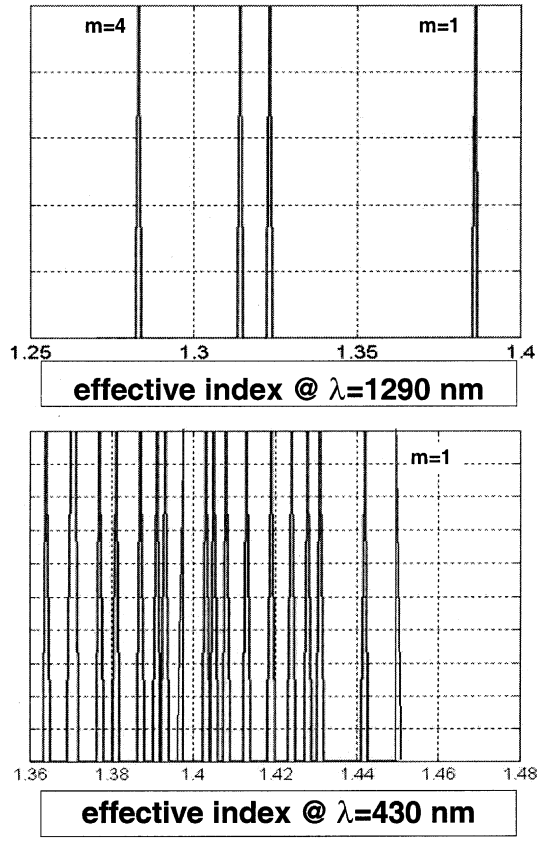

Fig. 7. Calculated effective index of lower-order modes at 1290 and 430 nm.

However, the experimental structure is more irregular, likely because the THG process involves more than one high-order mode.

In order to derive the phase-matching wavelength λ_m for the THG involving the mth order mode, we linearize the dependence of the effective refractive index on wavelength around both 1290 and 430 nm as

$$\begin{aligned} n^1_\lambda &= n^1_{1290} + \alpha_1(1290 - \lambda), \\ n^m_{\lambda/3} &= n^m_{430} + \alpha_m(430 - \lambda/3), \end{aligned} \tag{1}$$

where wavelengths are expressed in nanometers. The phase-matching condition gives the following expression for λ_m:

$$\lambda_m = 1290 + \frac{n^1_{1290} - n^m_{430}}{\alpha_1 - \alpha_m/3}. \tag{2}$$

The numerically calculated slopes for the fundamental mode around 1290 nm and for the 14th-order mode around 430 nm are: $\alpha_1 = 0.95 \times 10^{-4}$ nm^{-1}, and $\alpha_{14} = 5.85 \times 10^{-4}$ nm^{-1}. By making the simplifying assumption that the slopes α_{13} and α_{15} have the same value as α_{14}, we derive from Eq. (2) the following values for the phase-matching wavelengths: $\lambda_{13} = 1330$ nm, $\lambda_{15} = 1240$ nm. It is interesting to note that the detailed spectral structure of the observed blue light, as shown in Fig. 8, presents indeed two secondary peaks that roughly correspond to $\lambda_{13}/3$ and $\lambda_{15}/3$. It is very important to stress that the efficiency of the THG process is proportional to the overlap integral [11] between the cube of the field of the fundamental

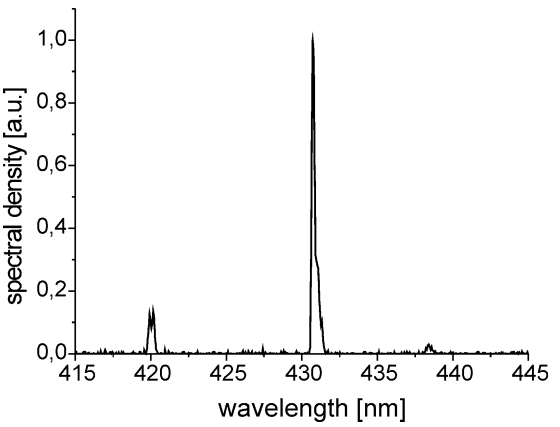

Fig. 8. Detail of the output spectrum obtained by launching 110-fs pulses at $\lambda = 1290$ nm: the observed lines correspond to third-harmonic generation on the 13th, 14th, and 15th mode.

(infrared) mode and the field of the higher-order (blue) mode. The value of the overlap integral may be strongly dependent on the mode order, so that one should not expect to find in the output spectrum peaks corresponding to all possible phase-matched interactions. We mentioned above, in connection with the description of Fig. 2, that a line corresponding roughly to the third harmonic of 1550 nm was also observed. By extrapolating somewhat arbitrarily Eq. (2), we would find that the phase-matching wavelength λ_9 could be around 1550.

3.2. Four-wave mixing

We discuss now the appearance of the 890-nm x-polarized line shown in the spectra of Fig. 4. Noting that such a spectral line is present in the output spectrum only when the polarization of the input field is not directed along a principal polarization axis, we argue that the 890-nm line arises from a four-wave mixing process involving off-diagonal terms of $\chi^{(3)}$. Therefore, the x- and z-components of the nonlinear polarization vector $\mathbf{P}_c$ can be expressed as

$$P_{cx} \div \chi_{xxzz} E_{sx} * E_{pz} E_{pz} = \chi_{xxzz} E_s E_p^2 \cos^2\theta \sin\theta, \qquad (3)$$

$$P_{cz} \div \chi_{zzxx} E_{sz} * E_{px} E_{px} = \chi_{zzxx} E_s E_p^2 \sin^2\theta \cos\theta, \qquad (4)$$

where E_p and E_s are, respectively, the "pump" and "signal" field having wavelength within the supercontinuum, E_{pz} is the component of E_p along z, and E_{sx} is the component of E_s along x. Similar relations could be written by involving χ_{xzxz} instead of χ_{xxzz}, and χ_{zxzx} instead of χ_{zzxx}. It is not possible to measure precisely the wavelength λ_p of the field E_p, but we can make a rough evaluation by monitoring at which value of spectral broadening of the supercontinuum the four-wave mixing process starts to be effective. We find that λ_p is in the range 1100–1150 nm.

Eq. (3) predicts that the 890-nm output power P_{890} is maximum when $\theta = 35°$. This is in agreement with our experimental results. In particular, there is internal consistency between the observation that the maximum of P_{890} corresponds to a value of θ around 35° and the finding that the 890-nm light has an x-polarization. On the contrary, Eq. (4) predicts a z-polarized 890-nm output beam with maximum power at a value of θ around 60°.

We verified experimentally that the fiber is at least bimodal at 890 nm. Such an observation is confirmed by our numerical simulation results. However, the calculated difference in effective index between the fundamental mode and the second-order mode is too large (see Fig. 6) to permit a phase-matching situation involving the second-order 890-nm mode. We did not measure the birefringence Δn of our fiber, but we can say that, considering the similarity with the fiber studied in [5], the value of Δn is around 10^{-3}. Taking into account the behavior of the effective index given in Fig. 6, we find that such a value is compatible with the hypothesis that the phase-matching mechanism for the observed four-wave mixing effect is guaranteed only by the fiber birefringence. Note that the two processes described by Eqs. (3) and (4) cannot be both phase-matched by the fiber birefringence. The sign of Δn determines which one of the two processes is phase-matched. Incidentally, we note that the influence of the input polarization on nonlinear interactions in holey fibers have also been studied in [4], but in a rather different context.

Sharping et al. [12] have recently reported the first experimental demonstration of non-degenerate four-wave mixing in a holey fiber by injecting both pump and signal with a linear polarization parallel to one of the principal axes of the fiber. However, their situation is different from ours because they operated near the zero-dispersion wavelength, and kept a very small (few nanometers) wavelength difference $\Delta\lambda$ between pump and signal. In our case, $\Delta\lambda$ is larger by two orders of magnitude, so that the phase-matching condition cannot be satisfied without exploiting the fiber birefringence.

4. Conclusions

As a conclusion, we have shown that various nonlinear interactions can start from the supercontinuum generated by ultrashort infrared pulses, giving rise to the generation of an intense

narrow-band signal in the blue through a third-harmonic generation process phase-matched by modal dispersion. In principle, every holey fiber should have several phase-matching wavelengths λ_m for the generation of a third-harmonic wave in the mth order mode. In our case, efficient THG is observed for only one value of m. We attribute this to the fact that only for that mode the overlap integral is significantly different from zero. Generally speaking, it is likely that, for most fiber structures, no overlap integral is large enough to give any THG.

The scenario is enriched when the input polarization is changed: a 890-nm line is generated by a four-wave mixing process that exploits non-diagonal components of the third-order susceptibility tensor and uses fiber birefringence to satisfy the phase-matching condition. Our data allow to identify which components are responsible for the observed process.

Acknowledgements

We thank D. J. Richardson and T. M. Monro for useful discussions.

References

[1] P. Petropoulos, T.M. Monro, W. Belardi, K. Furusawa, J.H. Lee, D.J. Richardson, Opt. Lett. 26 (2001) 1233.
[2] J.K. Ranka, R.S. Windeler, A.J. Stentz, Opt. Lett. 25 (2000) 25.
[3] S. Coen, A.H.L. Chau, R. Leonhardt, J.D. Harvey, J.C. Knight, W.J. Wadsworth, P.St.J. Russell, Opt. Lett. 26 (2001) 1356.
[4] S. Coen, A.H.L. Chau, R. Leonhardt, J.D. Harvey, J.C. Knight, W.J. Wadsworth, P.St.J. Russell, J. Opt. Soc. Am. B 19 (2002) 753.
[5] J.H.V. Price, W. Belardi, T.M. Monro, A. Malinowski, A. Piper, D.J. Richardson, Opt. Express 10 (2002) 382.
[6] J.M. Dudley, L. Provino, N. Grossard, H. Maillotte, R.S. Windeler, B.J. Eggleton, S. Coen, J. Opt. Soc. Am. B 19 (2002) 765.
[7] F.G. Omenetto, A.J. Taylor, M.D. Moores, J. Arriaga, J.C. Knight, W.J. Wadsworth, P.St.J. Russell, Opt. Lett. 26 (2001) 1158.
[8] A.V. Husakou, J. Herrmann, Phys. Rev. Lett. 87 (2001) 203901.
[9] J. Herrmann, U. Griebner, N. Zhavoronkov, A. Husakou, D. Nickel, J.C. Knight, W.J. Wadsworth, P.St.J. Russell, G. Korn, Phys. Rev. Lett. 88 (2002) 173901.
[10] J.K. Ranka, R.S. Windeler, A.J. Stentz, Opt. Lett. 25 (2000) 796.
[11] G.P. Agrawal, in: Nonlinear Fiber Optics, Academic Press, San Diego, 1995, p. 409.
[12] J.E. Sharping, M. Fiorentino, A. Coker, P. Kumar, R.S. Windeler, Opt. Lett. 26 (2001) 1048.